

~~C 30.70.63~~
~~ATSL~~

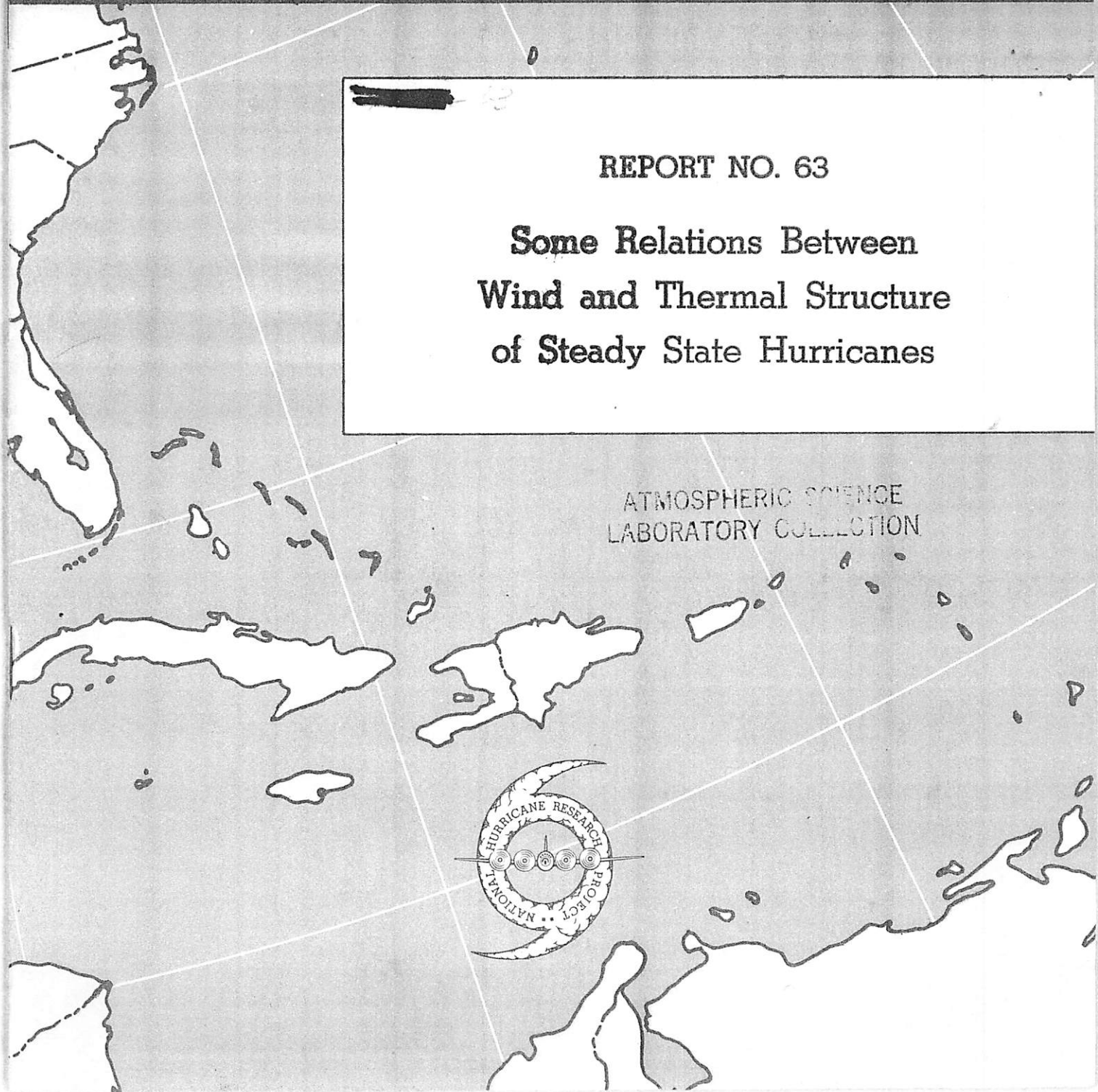
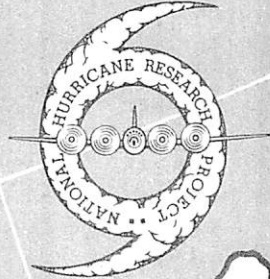
NATIONAL HURRICANE RESEARCH PROJECT

QC944
N39
10.63
ATSL

REPORT NO. 63

**Some Relations Between
Wind and Thermal Structure
of Steady State Hurricanes**

ATMOSPHERIC SCIENCE
LABORATORY COLLECTION



U. S. DEPARTMENT OF COMMERCE
Luther H. Hodges, Secretary
WEATHER BUREAU
F. W. Reichelderfer, Chief

NATIONAL HURRICANE RESEARCH PROJECT

REPORT NO. 63

Some Relations Between Wind and Thermal Structure
of Steady State Hurricanes

by

Herbert Riehl

Colorado State University, Fort Collins, Colo.



Washington, D. C.
June 1963



018401 0601206

NATIONAL HURRICANE RESEARCH PROJECT REPORTS

Reports by Weather Bureau units, contractors, and cooperators working on the hurricane problem are preprinted in this series to facilitate immediate distribution of the information among the workers and other interested units. As this limited reproduction and distribution in this form do not constitute formal scientific publication, reference to a paper in the series should identify it as a preprinted report.

- No. 1. Objectives and basic design of the NERP. March 1956.
- No. 2. Numerical weather prediction of hurricane motion. July 1956.
Supplement: Error analysis of prognostic 500-mb. maps made for numerical weather prediction of hurricane motion. March 1957.
- No. 3. Rainfall associated with hurricanes. July 1956.
- No. 4. Some problems involved in the study of storm surges. December 1956.
- No. 5. Survey of meteorological factors pertinent to reduction of loss of life and property in hurricane situations. March 1957.
- No. 6. A mean atmosphere for the West Indies area. May 1957.
- No. 7. An index of tide gages and tide gage records for the Atlantic and Gulf coasts of the United States. May 1957.
- No. 8. Part I. Hurricanes and the sea surface temperature field. Part II. The exchange of energy between the sea and the atmosphere in relation to hurricane behavior. June 1957.
- No. 9. Seasonal variations in the frequency of North Atlantic tropical cyclones related to the general circulation. July 1957.
- No. 10. Estimating central pressure of tropical cyclones from aircraft data. August 1957.
- No. 11. Instrumentation of National Hurricane Research Project aircraft. August 1957.
- No. 12. Studies of hurricane spiral bands as observed on radar. September 1957.
- No. 13. Mean soundings for the hurricane eye. September 1957.
- No. 14. On the maximum intensity of hurricanes. December 1957.
- No. 15. The three-dimensional wind structure around a tropical cyclone. January 1958.
- No. 16. Modification of hurricanes through cloud seeding. May 1958.
- No. 17. Analysis of tropical storm Frieda 1957. A preliminary report. June 1958.
- No. 18. The use of mean layer winds as a hurricane steering mechanism. June 1958.
- No. 19. Further examination of the balance of angular momentum in the mature hurricane. July 1958.
- No. 20. On the energetics of the mature hurricane and other rotating wind systems. July 1958.
- No. 21. Formation of tropical storms related to anomalies of the long-period mean circulation. September 1958.
- No. 22. On production of kinetic energy from condensation heating. October 1958.
- No. 23. Hurricane Audrey storm tide. October 1958.
- No. 24. Details of circulation in the high energy core of hurricane Carrie. November 1958.
- No. 25. Distribution of surface friction in hurricanes. November 1958.
- No. 26. A note on the origin of hurricane radar spiral bands and the echoes which form them. February 1959.
- No. 27. Proceedings of the Board of Review and Conference on Research Progress. March 1959.
- No. 28. A model hurricane plan for a coastal community. March 1959.
- No. 29. Exchange of heat, moisture, and momentum between hurricane Ella (1958) and its environment. April 1959.
- No. 30. Mean soundings for the Gulf of Mexico area. April 1959.
- No. 31. On the dynamics and energy transformations in steady-state hurricanes. August 1959.
- No. 32. An interim hurricane storm surge forecasting guide. August 1959.
- No. 33. Meteorological considerations pertinent to standard project hurricane, Atlantic and Gulf coasts of the United States. November 1959.
- No. 34. Filling and intensity changes in hurricanes over land. November 1959.
- No. 35. Wind and pressure fields in the stratosphere over the West Indies region in August 1958. December 1959.
- No. 36. Climatological aspects of intensity of typhoons. February 1960.
- No. 37. Unrest in the upper stratosphere over the Caribbean Sea during January 1960. April 1960.
- No. 38. On quantitative precipitation forecasting. August 1960.
- No. 39. Surface winds near the center of hurricanes (and other cyclones). September 1960.
- No. 40. On initiation of tropical depressions and convection in a conditionally unstable atmosphere. October 1960.
- No. 41. On the heat balance of the troposphere and water body of the Caribbean Sea. December 1960.
- No. 42. Climatology of 24-hour North Atlantic tropical cyclone movements. January 1961.
- No. 43. Prediction of movements and surface pressures of typhoon centers in the Far East by statistical methods. May 1961.
- No. 44. Marked changes in the characteristics of the eye of intense typhoons between the deepening and filling states. May 1961.
- No. 45. The occurrence of anomalous winds and their significance. June 1961.
- No. 46. Some aspects of hurricane Daisy, 1958. July 1961.
- No. 47. Concerning the mechanics and thermodynamics of the inflow layer of the mature hurricane. September 1961.
- No. 48. On the structure of hurricane Daisy (1958). October 1961.
- No. 49. Some properties of hurricane wind fields as deduced from trajectories. November 1961.
- No. 50. Proceedings of the Second Technical Conference on Hurricanes, June 27-30, 1961, Miami Beach, Fla. March 1962.
- No. 51. Concerning the general vertically averaged hydrodynamic equations with respect to basic storm surge equations. April 1962.
- No. 52. Inventory, use, and availability of NERP meteorological data gathered by aircraft. April 1962.
- No. 53. On the momentum and energy balance of hurricane Helene (1958). April 1962.
- No. 54. On the balance of forces and radial accelerations in hurricanes. June 1962.
- No. 55. Vertical wind profiles in hurricanes. June 1962.
- No. 56. A theoretical analysis of the field of motion in the hurricane boundary layer. June 1962.
- No. 57. On the dynamics of disturbed circulation in the lower mesosphere. August 1962.
- No. 58. Mean sounding data over the western tropical Pacific Ocean during the typhoon season. and Distribution of turbulence and icing in the tropical cyclone. October 1962.
- No. 59. Reconstruction of the surface pressure and wind fields of hurricane Helene. October 1962.
- No. 60. A cloud seeding experiment in hurricane Esther, 1961. November 1962.
- No. 61. Studies on statistical prediction of typhoons. April 1963.
- No. 62. The distribution of liquid water in hurricanes. April 1963.

QC 944
.N39
no. 63
ATSL

CONTENTS

	Page
ABSTRACT	1
1. INTRODUCTION	2
2. OCEANIC HEAT SOURCE AND SURFACE PRESSURE IN HURRICANES	2
3. MODEL OF HURRICANE WIND STRUCTURE	5
4. KINETIC ENERGY COMPUTATIONS	8
5. RADIAL TEMPERATURE DISTRIBUTION	10
6. HEAT SOURCE AND MOMENTUM SINK	14
Radial motion	14
Criterion for steady-state hurricane	15
7. EXAMINATION OF HURRICANE CASES	18
Hurricane Donna	20
Hurricane Daisy	20
Hurricane Helene	23
Hurricane Carrie	24
Hurricane Cleo	25
8. SUMMARY	26
ACKNOWLEDGMENT	27
REFERENCES	27

SOME RELATIONS BETWEEN WIND AND THERMAL STRUCTURE
OF STEADY STATE HURRICANES

Herbert Riehl
Colorado State University

ABSTRACT

Several simple integrations are performed to determine to what extent a steady, symmetrical hurricane model can be used to approximate observed storm structure.

A two-layer model with inflow and outflow is considered. In the outflow, the absolute angular momentum about the vertical axis at the hurricane center is conserved. In the inflow, conservation of potential vorticity is assumed. For specified outer boundary conditions this assumption determines the distribution of momentum transport from air to ocean and therewith the radial profile of the tangential wind component.

The local heat source at the ocean surface is assumed to supply the energy for the generation of hurricane winds. Given this heat source and the vertical wind shear between inflow and outflow layers from the dynamic model, a relation must exist between heat source and momentum sink at the air-water interface, if a particular wind field is to exist in steady state. This relation is computed.

Various empirical tests are performed to assess the degree of reality of the model. Observations from hurricanes between 1945 and 1958 are used. Most observational material is taken from research missions conducted by aircraft of the National Hurricane Research Project. It is found that the crude model gives a rather good approximation to several hurricanes, especially the more intense ones. But it cannot explain all measurements taken by NHRP; of course, steady state did not exist in all situations investigated by aircraft.

It may be concluded that computations with steady, symmetrical models are relevant at least to partial understanding of hurricanes.

1. INTRODUCTION

In a recent paper Malkus and Riehl [7] computed inflow trajectories into steady state hurricanes through integration of simplified equations of motion. They then related this low-level model to oceanic heat source distribution and to atmospheric energy budget requisite for maintaining a steady storm.

The aim of this paper, following [7] and Haurwitz [3], is to describe, in quantitative terms, some features of tropical storm circulations observed in a large fraction of cases. The particular problem to be discussed is this: In hurricanes, the cyclonic tangential wind component decreases upward, especially above the middle troposphere. This decrease, at any particular radius, must be related to the transfer of angular momentum from air to ocean inside this radius. Further, given essentially the appropriate thermal wind relationship, the vertical shear of the tangential wind also must be related to the radial temperature gradient and, in turn, to the oceanic heat source thought to be mainly responsible for the existence of lateral temperature gradients inside hurricanes. Thus, there must be some relations between heat source and momentum sink in the hurricane interior, so that a particular wind field can exist in steady state.

These relations will be explored with simple and approximate integrations. The problem, as posed, demands that the earlier one-layer investigation be extended at least to two layers: the inflow and outflow regimes. An essential assumption made in the previous work is retained -- that of a steady symmetrical vortex. Though research aircraft missions and synoptic data have demonstrated important asymmetries and meso-structural details of hurricanes, the symmetrical model remains attractive because of its simplicity and because the extent to which hurricane structure can be computed with this model has not been ascertained.

The presentation is divided into the following parts:

- (1) Evidence for a relation between oceanic heat source and surface pressure distribution.
- (2) Specification of the tangential velocity field; kinetic energy computations.
- (3) Relation between maximum wind, vertical wind shear, and heat source.
- (4) Relation between heat source and momentum sink for steady velocity fields.
- (5) Comparison of computed and observed hurricane structure.

2. OCEANIC HEAT SOURCE AND SURFACE PRESSURE IN HURRICANES

Given a troposphere with moist-adiabatic stratification up to the level of zero buoyancy relative to a mean tropical atmosphere of summer (Jordan [4]), Malkus and Riehl [7] integrated the hydrostatic equation from 100 mb. - assumed undisturbed - to the surface over a limited range of equivalent potential temperatures (θ_e) of interest for hurricane calculations. With these specifications the hydrostatic equation can be written

$$-\delta p_s = 2.5 \delta \theta_e \quad (1)$$

where p_s is surface pressure expressed in mb. and θ_e is in degrees K. The applicability of this relation, first used to correlate radial gradients of p_s and θ_e in a given storm, can be applied to a comparison of different storms. As evidenced by the great majority of research missions undertaken by the National Hurricane Research Project of the United States Government, the wall cloud of hurricanes is almost vertical; nearly constant θ_e with height may be expected there. On a number of research missions a B-47 aircraft operated by the U. S. Air Force penetrated the wall cloud at 235-250 mb. The temperature reading in cloud at the inner edge of the wall should give the warmest temperature and also the highest θ_e in a storm derived through heat transfer from sea to air in the storm. Miss Margaret Chaffee, Woods Hole Oceanographic Institution, determined these θ_e values for all available cases using all existing observational tools for the specification.

The θ_e values may be related to surface pressure at the inner edge of the eye wall. In practice, central pressures are obtained from dropsonde observations inside an eye where, on occasion, pressure may be considerably lower than in the eye wall. The pressure decrease from eye wall to eye interior is without interest for purposes of this paper. The mass circulating from the outside through the rain area does not move through this pressure drop which, therefore, is not utilized for the generation of wind energy. In several cases, notably hurricane Helene (1958), pressure at the eye wall (p_c) was estimated as closely as possible with present tools of observation. Because the pressure profile is so steep in just this part of hurricanes, only a first approximation can be expected; it may be that surface pressures, as finally estimated, are still a little low.

Figure 1 shows the relation between p_c and θ_e , with the variables determined as just described. Evidently there is a good correlation. The question is how the slope of the linear regression line compares with that to be expected according to the hydrostatic relation expressed in equation (1). It is found that

$$p' = - 2.56 \theta_e'$$

where p' is the pressure departure from 1005 mb. and θ_e' is the departure from 350°k. The result is satisfactory and demonstrates that the eye wall pressure variation of different storms is produced indeed by variation in oceanic heat source strength.

We now wish to relate this heat source to the wind structure of hurricanes. Toward this end we shall at first compute a simple model of the distribution of the tangential wind component.

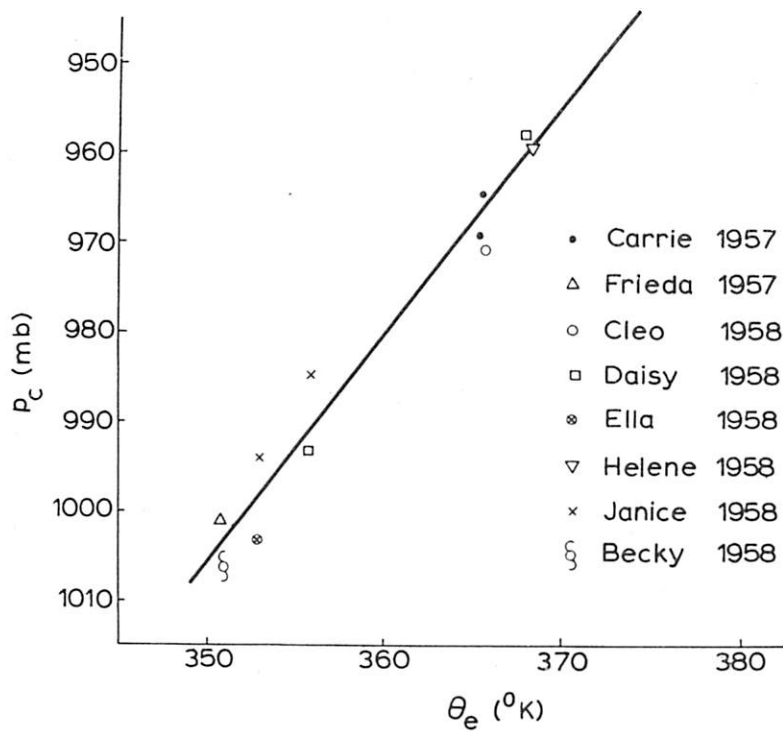


Figure 1. - Equivalent potential temperature ($^{\circ}\text{K}$.) observed by B-47 aircraft flying at 235-250 mb. in cloud at inner eye wall of indicated tropical storms and hurricanes vs. pressure (mb.) at rim of eye.

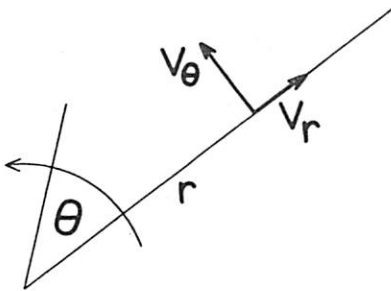


Figure 2. - Illustrating polar coordinate system used.

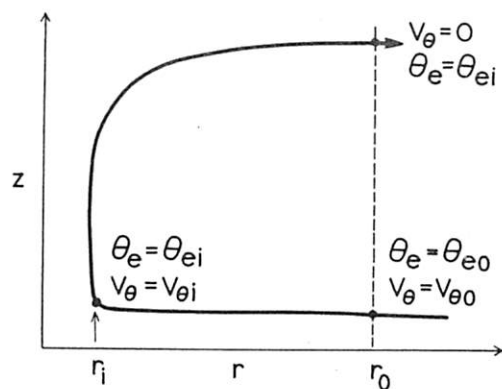


Figure 3. - Illustrating hurricane mass circulation. For meaning of symbols see text.

3. MODEL OF HURRICANE WIND STRUCTURE

The equations of motion in polar coordinates, neglecting lateral friction, are expressed by

$$\frac{dv_{\theta}}{dt} + \frac{v_{\theta}v_r}{r} + fv_r = -\frac{1}{\rho} \frac{\partial p}{r\partial\theta} + \frac{1}{\rho} \frac{\partial \tau_{\theta z}}{\partial z}, \quad (2)$$

$$\frac{dv_r}{dt} - \frac{v_{\theta}^2}{r} - fv_{\theta} = -\frac{1}{\rho} \frac{\partial p}{\partial r} + \frac{1}{\rho} \frac{\partial \tau_{rz}}{\partial z}. \quad (3)$$

Notation is as follows: v_{θ} and v_r are tangential and radial wind components positive along θ and r (fig. 2); t is time, z height, ρ density, f the Coriolis parameter, $\tau_{\theta z}$ the shearing stress in the $\theta - z$ plane and τ_{rz} the corresponding stress in the $r - z$ plane. The absolute angular momentum per unit mass about the vertical axis at the center of the hurricane

$$\Omega = v_{\theta}r + \frac{fr^2}{2}$$

assuming constant Coriolis parameter over the short radial distances involved. Noting that

$$\frac{d\Omega}{dt} = r \frac{dv_{\theta}}{dt} + v_{\theta}v_r + rfv_r,$$

the first equation of motion, written as momentum equation for the symmetrical vortex, becomes

$$\frac{d\Omega}{dt} = \frac{r}{\rho} \frac{\partial \tau_{\theta z}}{\partial z}. \quad (4)$$

For the balance of forces in the radial direction we shall write merely

$$\frac{v_{\theta}^2}{r} = g \frac{\partial h}{\partial r}. \quad (5)$$

when referred to isobaric coordinates, where g is acceleration of gravity and h the height of an isobaric surface. These formulations are considered to be adequate statements of the situation for the present objectives. It may be noted that direct use of equation (5) for computation of the temperature field through the thermal wind approach is unsatisfactory. This would involve evaluation of

$$\int \partial v_{\theta}^2 / \partial z \delta l_{nr},$$

which cannot be done directly. Instead, we shall approach the problem with the simple and crude model of figure 3 which features a lower inflow and an upper outflow layer. Whenever a model of this type really holds, Ω must decrease upward since momentum is given off to the ocean along the entire inflow path. This will be true even for weak tropical cyclones, as long as equations (4) and (5) adequately express the principal dynamic relations. It should be noted that at the eye wall, with completely vertical ascent,

$\partial v_{\theta}^2 / \partial z = 0$, implying that the radial temperature gradient vanishes there. This is not true and constitutes one of the inconsistencies of the model held unimportant for this study.

We shall be concerned with the region between r_i and r_o in figure 3, where r_i denotes the radius of maximum wind ($V = v_{\theta}$) and r_o denotes the radius where, in the outflow, $v_{\theta} = 0$, i.e., the radius where cyclonic circulation changes to anticyclonic circulation in the upper troposphere. We shall assume equation (5) to hold for both inflow and outflow layers. Further, for the inflow equation (4) will be used, while for the outflow we shall set

$$\frac{d\Omega}{dt} = 0. \quad (6)$$

As shown by Kleinschmidt [5] and Riehl and Malkus [11], conservation of absolute angular momentum is a reasonable first approximation in the outflowing mass.

Outflow layer: From equation (6) it follows directly that

$$\frac{f r_o^2}{2} = v_{\theta i} r_i + \frac{f r_i^2}{2}. \quad (7)$$

Limiting consideration to cases where $f r_i \ll v_{\theta i}$, this expression may be approximated by

$$r_o = \left(\frac{2}{f} v_{\theta i} r_i \right)^{1/2}. \quad (8)$$

Inflow layer: Equation (4) may be integrated over an inflow layer of depth δz at the top of which $\tau_{\theta z} = 0$. Then

$$\int \frac{d\Omega}{dt} \rho \delta z = - r \tau_{\theta s}, \quad (9)$$

where $\tau_{\theta s}$ is the surface tangential stress component.

It is well known that the absolute vorticity increases in the converging inflow into hurricanes, suggesting that the principle of conservation of potential vorticity may hold in the first approximation. Riehl and Malkus [11] showed this to be correct, within computational limits, for the inflow into hurricane Daisy (1958). If conservation of potential vorticity is assumed, the curl of the component of the frictional force along θ must be zero. This component $F_{\theta} = 1/\rho \partial \tau_{\theta z} / \partial z$. Taking $\nabla \times F_{\theta} = 0$ and noting that the component of the ∇ -operator applicable along r is $1/r \partial / \partial r (r \quad)$, we have $F_{\theta} r = \text{const}$. Integrating with height from the surface to the level where the stress vanishes,

$$r \tau_{\theta s} = \text{const}. \quad (10)$$

Empirically, a relation of the form $r^m \tau_{\theta s} = \text{const}$ has been found to hold well for individual storms and for mean hurricanes (Palmén and Riehl [8]). Here m is an exponent with observed range from somewhat greater than 1 to somewhat less than 1. In this paper we shall set $m = 1$ as a suitable mean value and accept equation (10).

The surface stress commonly is expressed as dependent on the square of the surface wind,

$$\tau_{\theta s} = C_D \rho_s v_{\theta s}^2 / \cos \alpha, \quad (11)$$

where C_D is the drag coefficient, ρ_s density at the surface, $v_{\theta s}$ the tangential wind component measured at ship's deck level, and α the inflow angle. Since, in the mean, this angle averages only about 15° around hurricanes (Ausman [1]), we shall set $\cos \alpha = 1$ for the computations here contemplated.

Equation (11) can be used only with reservations. Evidence has accumulated suggesting that C_D rises toward the interior of hurricanes. This evidence, however, is based on computations with pyramiding assumptions; there is not a single observation to prove whether the increase is realistic. In this paper we regard C_D as constant, noting as in the case of our other assumptions, that the conclusions will have to be modified should later data show that this step of convenience affects the outcome of the calculations materially.

Combining equations (10) and (11)

$$r v_{\theta}^2 = \text{const.}$$

or

$$v_{\theta} r^{1/2} = \text{const.} \quad (12)$$

This relation gives a good approximation of v_{θ} - r profiles found by investigators of many tropical storms around the globe.

At the radius of maximum wind, r_i , the inner boundary condition demands that the tangential speed $v_{\theta i}$ must be the same for inflow and outflow. Therefore, evaluating the constant in equation (12) at $v_{\theta} = v_{\theta i}$, $r = r_i$, and combining with equation (8), the radius of innermost penetration of the inflow is given by

$$r_i = \frac{r_o^3 f^2}{4v_{\theta o}^2}, \quad (13)$$

where $v_{\theta o}$ is the tangential velocity component of the inflow at $r = r_o$. The associated maximum speed

$$v_{\theta i} = \frac{2v_{\theta o}^2}{f r_o} \quad (14)$$

Figure 4 shows r_i and $v_{\theta i}$ as functions of r_o and $v_{\theta o}$. We see, for a given value of r_o , that r_i decreases with increasing $v_{\theta o}$ and that $v_{\theta i}$ increases correspondingly. This result is requisite since more momentum must be given off to the ocean with increasing values of $v_{\theta o}$.

Both r_i and $v_{\theta i}$ are dependent on latitude. As example, these quantities have been plotted against latitude in figure 5 for $r_o = 200$ km., $v_{\theta o} = 20$ m./sec. Holding this outer boundary condition constant, the eye radius widens and the central speed diminishes as latitude increases. This is in accord with observations. The reason for the relation stems from the fact that the inflow angle, for given $v_{\theta o}$ and r_o , decreases with latitude. As a result, the trajectory winds inward more slowly at high than at low latitudes and the inward penetration required to effect the transfer of momentum to the ocean is smaller.

4. KINETIC ENERGY COMPUTATIONS

As our next step we shall determine the height gradient of isobaric surfaces in inflow and outflow layers between r_i and r_o . For the outflow this quantity is readily given if the kinetic energy equation for steady, frictionless flow is determined from equations (2) and (3) with the assumptions previously stated. Then, choosing isobaric coordinates,

$$\frac{v_{\theta i}^2}{2} = g (h_o - h_i)_u, \quad (15)$$

where the subscript u denotes the upper layer.

For the inflow we have, from equation (12),

$$v_{\theta}^2 = v_{\theta i}^2 \frac{r_i}{r}.$$

Entering this expression in equation (5)

$$v_{\theta i}^2 \frac{r_i}{r^2} = g \frac{\partial h}{\partial r}.$$

Since h is a function of r alone in this expression, we may integrate between r_i and r_o . Then

$$v_{\theta i}^2 \frac{r_o - r_i}{r_o} = g (h_o - h_i)$$

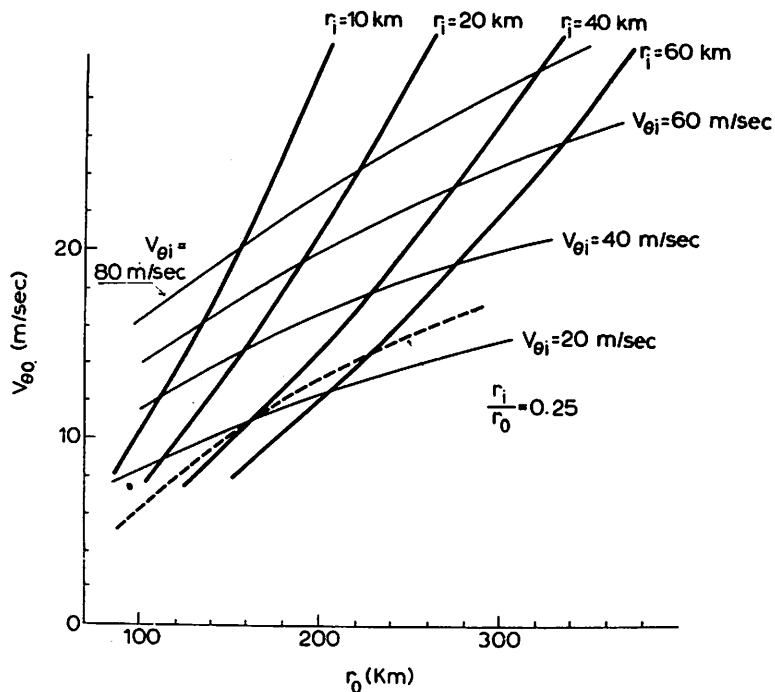


Figure 4. - Maximum speed (v_{θ_i}) and width of eye (r_i) as function of r_0 and v_{θ_0} at latitude 28° .

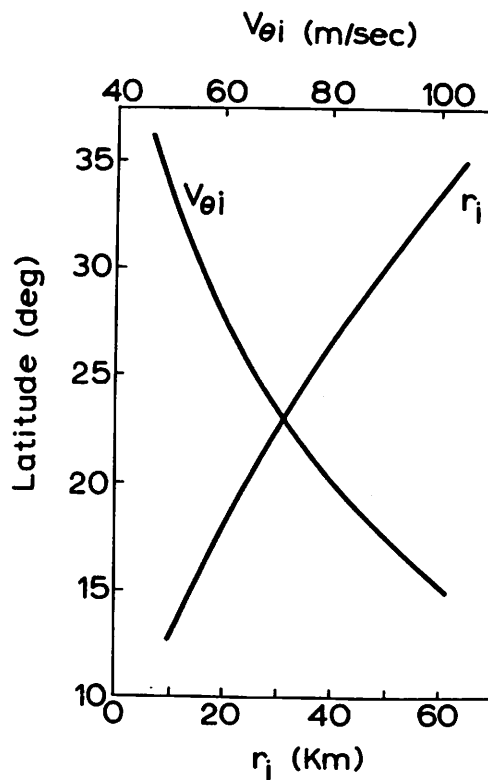


Figure 5. - Maximum speed (v_{θ_i}) and width of eye (r_i) as function of latitude for $r_0 = 200$ km., $v_{\theta_0} = 20$ m./sec.

and, for $r_i \ll r_o$,

$$v_{\theta i}^2 = g (h_o - h_i)_l \quad (16)$$

where the subscript l denotes the lower layer.

Comparing both layers, the slope of an isobaric surface in the outflow is just half of that in the inflow layer. Since $h_o - h_i$ measures the production of kinetic energy it follows that, in the inflow, half of the pressure work done is actually used to generate kinetic energy, while the other half is needed to balance frictional dissipation. This is an outcome of the analysis which can be tested, at least within limits, from observations. All hurricanes approaching the coast of the United States since 1940 were examined as to the availability of off-shore or coastal lighthouse observations that could be used to construct surface air trajectories from the periphery into a hurricane center. An essential criterion was the existence of a wind and pressure observation near the ring of strongest wind, or ability to assign a central pressure and maximum wind from other information such as aircraft reconnaissance reports. Usable trajectories could be constructed for only four storms:

September 14-15, 1945, off southeastern Florida (2 trajectories)

July 24, 1959, off Texas coast (2 trajectories)

September 9-10, 1960, off Florida Keys (1 trajectory)

September 26, 1958, off Carolina coast (1 trajectory).

Figure 6 shows the relation between production and actual generation of kinetic energy for these six trajectories. Clearly, the 2:1 ratio of production to actual generation holds well. Though figure 6 applies to individual trajectories rather than to averages around hurricanes, the good fit nevertheless may be cited in support of equation (16).

5. RADIAL TEMPERATURE DISTRIBUTION

We are now in a position to approach the core of the problems posed in the Introduction. From equations (15) and (16)

$$(h_o - h_i)_l = 2 (h_o - h_i)_u .$$

Defining $D = h_u - h_l$, the thickness between isobaric surfaces,

$$D_o - D_i = - (h_o - h_i)_u = - \frac{1}{2} (h_o - h_i)_l .$$

If \hat{T} is the mean virtual temperature between two isobaric surfaces, variation of the hydrostatic relation between two constant pressure surfaces yields

$$\frac{\delta \hat{T}}{\hat{T}} = \frac{\delta \hat{D}}{\hat{D}} = \frac{(h_o - h_i)_u}{\hat{D}} ,$$

where the "hat" denotes mean values between inflow and outflow layers and δ is defined positive toward decreasing radius. Using now equation (15)

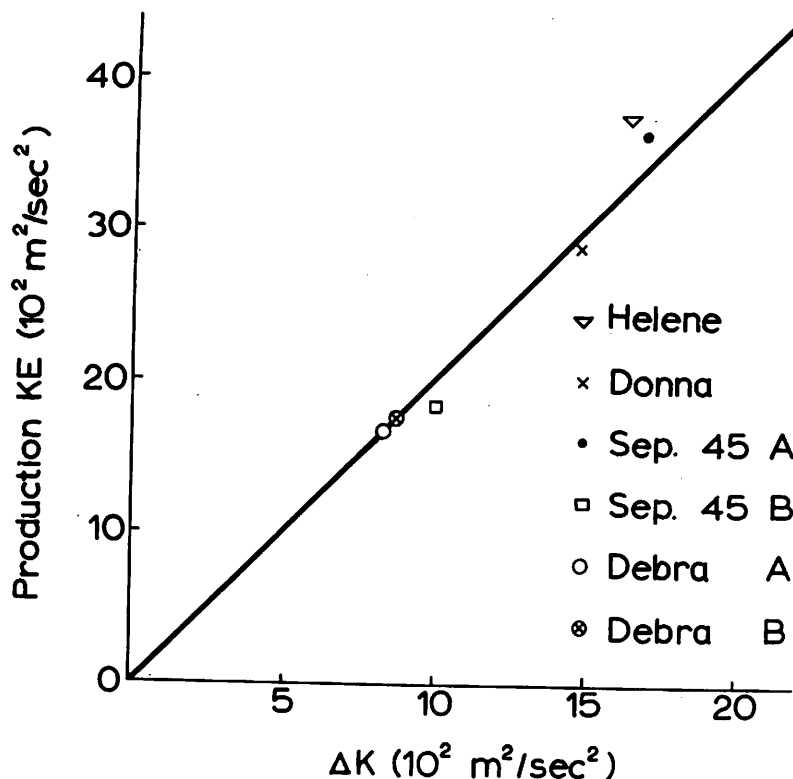


Figure 6. - Correlation between production of kinetic energy by pressure work (ordinate) against actual increase of kinetic energy of air (abscissa) as computed from trajectory calculations using lighthouse data near the United States coast for the indicated hurricanes.

$$v_{\theta i} = \left(2 g \frac{\hat{D}}{\hat{T}} \delta T \right)^{1/2} \quad (17)$$

and

$$v_{\theta i} = 27 (\delta \hat{T})^{1/2}, \quad (18)$$

when $\hat{D} = 10 \text{ km.}$, $\hat{T} = 270^\circ\text{K.}$, and $v_{\theta i}$ is expressed in m./sec. From equation (18) a temperature rise of only 1°K. will be associated with tropical storm speeds, showing the importance of even small temperature variations for tropical cyclones. However, because of the square-root relation, a 50 m./sec. storm requires a 4°K. temperature difference, while for an extreme typhoon of 100 m./sec., 14°K. is needed. Herewith, an upper limit of hurricane intensity and the difficulty in producing extreme hurricanes is clearly indicated, since the oceanic heat source must be relied upon to generate the required mean temperature difference.

Next we shall relate maximum wind and $\delta\theta_e$ with equation (1). Converting pressure gradient to height gradient of an isobaric surface in the inflow layer,

$$-g \rho \delta z_{\ell} = 2.5 \times 10^3 \delta \theta_e,$$

where the factor of 10^3 is needed to convert equation (1) to cgs units.

Then

$$g \rho (h_o - h_i)_{\ell} = 2.5 \times 10^3 (\theta_{ei} - \theta_{eo})$$

and

$$V_{\max}^2 = v_{\theta i}^2 = 2 \times 10^6 (\theta_{ei} - \theta_{eo}) \quad (19)$$

using standard density. Finally,

$$v_{\theta i} \text{ [m./sec.]} = 14.1 (\theta_{ei} - \theta_{eo})^{1/2}, \quad (20)$$

where it should be mentioned again that θ_e is the tropospheric mean value whereas \hat{T} in equation (18) refers to the thickness between inflow and outflow layers.

Equation (20) is graphed in figure 7 where θ_e , p' , and p_s scales also have been added for entering actual storm data. The θ_e values for four hurricanes, excluding Donna, are taken from figure 1; the method for computing V_{\max} is described in the last section of this paper. All observed points lie to the left of the theoretical values, indicating that the hurricanes failed to attain the central wind speeds demanded by the model. However, verification to the right of the dashed line is considered good, especially when one notes that all verifying winds were obtained by aircraft flying well above the main surface inflow layer. While the tangential component in hurricanes is fairly constant through the lower 20,000 ft. there is nevertheless, some decrease so that V_{\max} actually measured at, say, 3,000 ft. elevation should have been closer to the values demanded by figure 7.

The several hurricanes will be discussed in more detail later, when the large departures of maximum wind from the predicted maximum for Cleo and for Carrie (September 15) will also be examined. For the present it may be of interest to observe that tropical storm intensity ($V_{\max} = 20$ m./sec.) is indicated for $\theta_e = 352^\circ\text{K}$., $p_s = 1000$ mb. Such values of θ_e and p_s are produced when the mean tropical atmosphere of summer is replaced by an atmosphere corresponding to the parcel ascent of undisturbed trade wind air (Riehl [10]). The therefore mark a threshold; coincidence of these threshold values with cyclones of tropical storm intensity in steady state have been observed on numerous occasions. For lower pressure and hurricane force winds the oceanic heat source must be responsible as indicated by a rise of θ_e above 350 - 352°K .

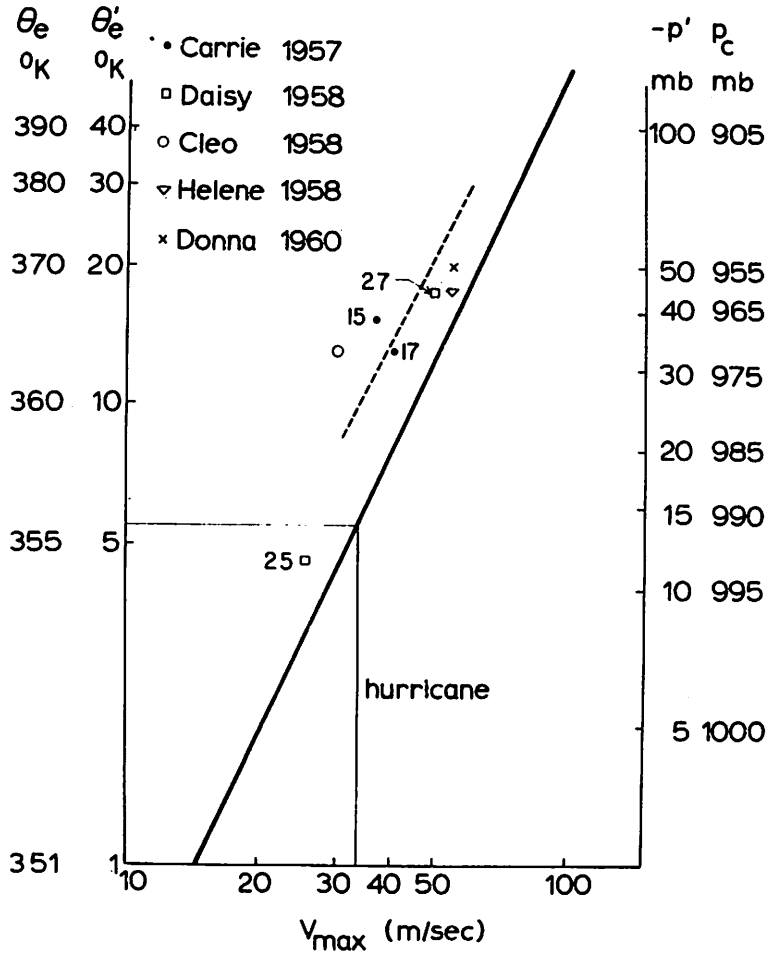


Figure 7. - Relation between maximum speed and increase of equivalent potential temperature according to equation (20) and comparison with the indicated hurricane cases. Scales of p_s and θ_e from figure 1.

6. HEAT SOURCE AND MOMENTUM SINK

Radial motion: Integrating equation (9) over a shallow inflow layer of thickness dz , over which Ω is taken as constant,

$$\Omega(t) - \Omega(t_0) = \text{const.} (t - t_0).$$

We shall set $t = t_0$ at $r = r_0$. There the momentum is $v_{\theta 0} r_0 + fr_0^2/2$. If the inflow reaches $r = r_i$ at time t , its momentum there will be $fr_0^2/2$ from equation (7). Thus $\Omega(t) - \Omega(t_0) = -v_{\theta 0} r_0$. The time needed for air to pass from r_0 to r_i may now be computed after introducing equation (11) into the constant and setting $t = 0$ at $r = r_0$. Then

$$t[\text{hours}] = 100/v_{\theta 0}, \quad (21)$$

where $C_D = 2.5 \times 10^{-3}$, $\Delta z = 1 \text{ km.}$; and $v_{\theta 0}$ is expressed in m./sec. This interesting relation states that the stronger the peripheral tangential velocity component, the shorter the time needed for air to pass from r_0 to r_i . For $v_{\theta 0} = 10 \text{ m./sec.}$, $t = 10 \text{ hours}$; for $v_{\theta 0} = 20 \text{ m./sec.}$, $t = 5 \text{ hours}$. Since, holding r_0 and f constant, r_i decreases and $v_{\theta i}$ increases with $v_{\theta 0}$, a strong storm requires a faster mass circulation through it than a weak storm.

It is of interest to determine whether the fast mass circulation is already found at r_0 and therewith enters into the boundary conditions. The space-time relation is obtained by differentiating equation (9) after substituting for v_{θ} from equation (12) and for the surface stress from equation (11). Thus,

$$\frac{d}{dt} \left(v_{\theta} r + \frac{fr^2}{2} \right) = \frac{d}{dt} \left(v_{\theta 0} r_0^{1/2} r^{1/2} + \frac{fr^2}{2} \right) = -\frac{C_D}{\Delta z} r_0 v_{\theta 0}^2.$$

Differentiating and solving for dt ,

$$-\frac{\Delta z}{C_D} \left[\frac{r^{-1/2}}{2r_0^{1/2} v_{\theta 0}} + \frac{fr}{r_0 v_{\theta 0}^2} \right] dr = dt, \quad (22)$$

where dr here is taken from an outer toward an inner radius. Defining $dr/dt \equiv v_r$ and evaluating at r_0 ,

$$-v_{r0} = \frac{C_D}{\Delta z} \frac{2r_0 v_{\theta 0}^2}{v_{\theta 0} + 2r_0 f}, \quad (23)$$

where v_{r0} denotes the radial velocity at r_0 . Clearly, v_{r0} will increase with $v_{\theta 0}$. For example, take $r_0 = 200 \text{ km.}$, $v_{\theta 0} = 15 \text{ m./sec.}$, which is close to the values observed in several storms. Then $v_{r0} = -4 \text{ m./sec.}$ and the inflow

angle $\alpha = 16^\circ$. This angle is near the average found by Ausman [1] for six hurricanes of 1954 and 1955. Given $r_o = 200$ km. and $v_{\theta o} = 20$ m./sec., $v_{r o} = -10$ m./sec. and $\alpha = 26^\circ$. From computations of v_r and α along several trajectories with equation (22) it is found that α at first is constant and then decreases. Mean values of 10° - 20° are obtained for the practical range indicated by observations in storms. Thus the approximation $\cos \alpha = 1$, made earlier, is justified.

Equation (23) may be tested further by relating $v_{r o}$ to central pressure. For this purpose $v_{r o}$ was computed at $r_o = 200$ km. for values of $v_{\theta o}$ ranging from 10 to 20 m./sec. This corresponds to a range of $v_{\theta i}$ from 20 to 80 m./sec. at latitude 20° . Using equations (1) and (19) the associated central pressure depression was found. Then this pressure depression was plotted against radial mass flow represented by $v_{r o} r_o$. We may compare the result with a correlation between mass inflow and central pressure determined empirically by Krueger [6]. Figure 8 shows the comparison after conversion of δp to p_c by setting our value equal to Krueger's at 965 mb. Although the possibility of a best fit with a curve rather than with a straight line was recognized at the time of Krueger's study, Krueger chose a linear regression lacking a physical hypothesis for a higher order solution. As evident from figure 8, our curve fits the data well and gives a better approximation than the straight line. It may be added that checks performed on the Krueger correlation with storm inflow data subsequent to 1955 have given generally satisfactory results.

Criterion for steady-state hurricane: As mentioned in the Introduction, a particular relation must exist between heat source and momentum sink in the interior of hurricanes, if a given velocity field is to be observed in steady state. Enhancement of transfer coefficients apart, the momentum sink is proportional to v_θ^2 (equation 11), while the heat source is proportional to v_θ , again setting $\cos \alpha = 1$. Hence it should not be possible to obtain a steady storm for any combination of r_o and $v_{\theta o}$. This question will now be investigated.

The total heat source Q_a over a trajectory with duration $(t_2 - t_1)$, following turbulence theory, is

$$Q_a = c_p \int (\theta_{e2} - \theta_{e1}) \rho \delta z = \int_{t_1}^{t_2} \frac{\rho_s C_D c_p}{\cos \alpha} E v_\theta dt, \quad (24)$$

if the heat gained from the ocean is obtained in the inflow layer. In equation (24) $E = (T_w - T_a) + L/c_p (q_w - q_a)$, where T_w and q_w are temperature and specific humidity at the sea surface; T_a and q_a are the same quantities at ship's deck level, and L is latent heat of evaporation. From previous work

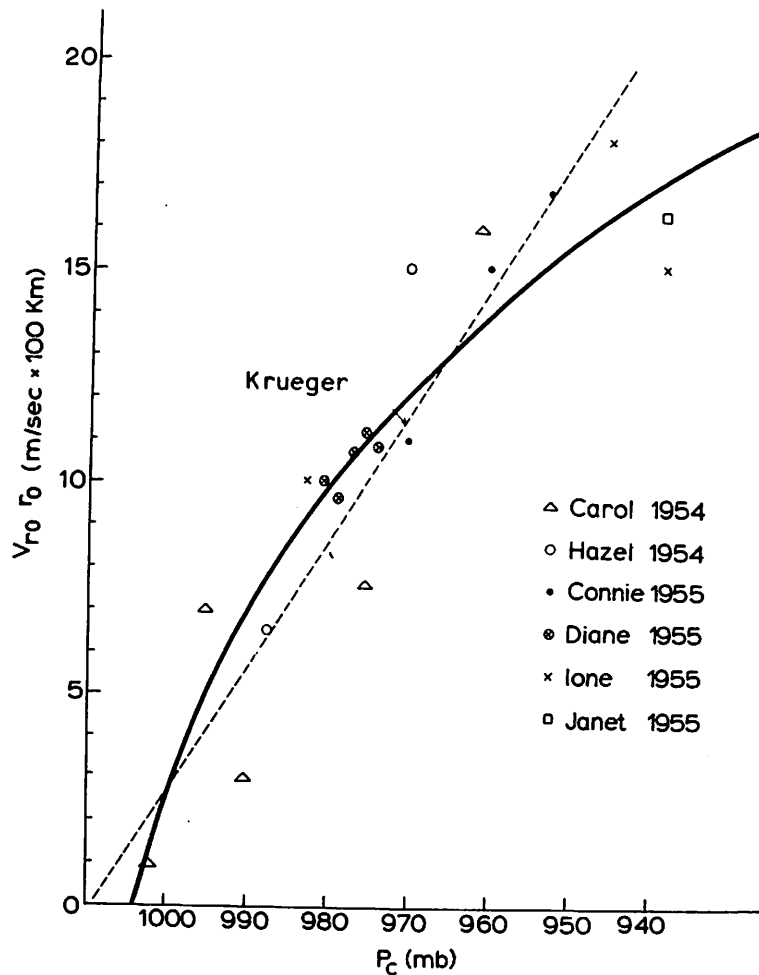


Figure 8. - Curve relating mass inflow (equation (23)) and central pressure. Data for six hurricanes and linear regression line from Krueger [6].

(cf. Malkus and Riehl [7]) $T_a - T_w$ approaches a constant value of about $2^\circ - 3^\circ\text{K}$. at pressures roughly below 995-1000 mb., so that the inward-moving air expands isothermally. The specific humidity difference $q_w - q_a$ slowly decreases inward as the moisture in the inflow increases. Within the limits here desired it will suffice to treat E parametrically, although an analytic expression could be formulated. This is not considered profitable until much improved knowledge on the actual air-sea heat and moisture exchange is obtained. With the assumption that E may be treated as constant over the inner region and holding $\theta_{e2} - \theta_{e1}$ constant over δz ,

$$\theta_{e2} - \theta_{e1} = \frac{C_D}{\Delta z} E \int v_\theta dt, \quad (25)$$

where the small difference between ρ and ρ_s also has been neglected. As

seen from figure 7 and other known cases, the wind speed corresponding to pressures of 995-1000 mb. roughly lies in the range of 20-30 m./sec. We shall choose here an average value of $v_{\theta h} = 25$ m./sec. at radius $r = r_h$, determined graphically, where equation (25) is assumed to become valid. Of course, there is heat flow from the ocean at lower speeds; the heat source is not likely to have a sudden onset at some threshold value of wind speed. However, this outer heat source is small compared to the inner heat source in hurricanes, and it has not been explored theoretically. For the purpose here at issue -- whether or not large heat exchange will materialize in the interior -- it appears justified to neglect the outer heat source.

We can now integrate equation (25) from r_h to r_i substituting for v_{θ} from equation (12) and for dt from equation (22). Then

$$\theta_{ei} - \theta_{eh} = E \left[\frac{1}{2} \ln \frac{r_h}{r_i} + \frac{2}{3} \frac{f (r_h^{3/2} - r_i^{3/2})}{v_{\theta h} r_h^{1/2}} \right]. \quad (26)$$

We may neglect $r_i^{3/2}$ compared to $r_h^{3/2}$ for all but very small differences between r_h and r_i . Introducing equation (19)

$$v_{\theta i}^2 = 10^2 E \left[\ln \frac{r_h}{r_i} + \frac{4}{3} \frac{f r_h}{v_{\theta h}} \right], \quad (27)$$

where $v_{\theta i}$ is expressed in m./sec. This relation gives the maximum speed as obtained through the operation of the heat source. Results are to be compared with $v_{\theta i}$ as required by equation (14). We may find that $v_{\theta i}$ as demanded by momentum balance exceeds the maximum speed that can be provided by the heat source. Then steady state cannot exist. Conversely, when air arrives at r_i with greater $v_{\theta i}$ through the heat source than is needed for momentum balance, the steady state condition again is violated. For each f and r_o there is only a single value of $v_{\theta o}$ which permits steady state (fig. 9).

For the construction of figure 9 we have chosen $E = 12.5^\circ\text{K.}$ using $T_w - T_a = 2.5^\circ\text{K.}$ and $q_w - q_a = 4$ g./kg. as found in hurricane Daisy (1958) in the inner area. This value of E will be applied to all storms. Evidently, some variation of results can be obtained depending on the choice of the air-sea interaction parameters $v_{\theta h}$ and E .

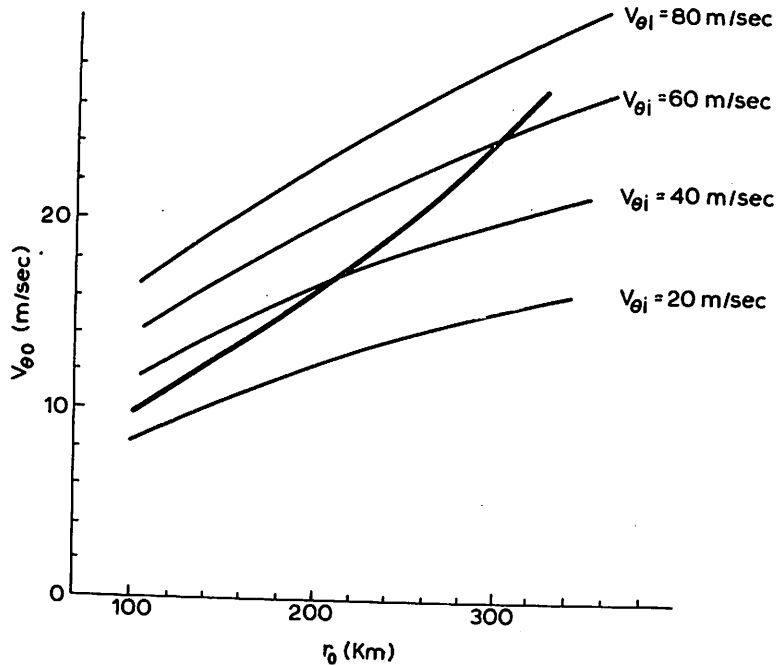


Figure 9. - Limiting curve for r_0 and $v_{\theta 0}$ satisfying steady state condition (heavy) and maximum speeds at latitude 28° from figure 4.

7. EXAMINATION OF HURRICANE CASES

In the Atlantic hurricane area the number of situations with sufficient observations for testing the validity of the model presented is very small indeed. Data sources are the research flights made by the National Hurricane Research Project and the observations of the West Indies rawinsonde network. Only the following days qualify for a check:

Carrie (September 15 and 17, 1957)
 Daisy (August 25 and 27, 1958)
 Cleo (August 18, 1958)
 Helene (September 26, 1958)
 Donna (September 7, 1960)

The symmetrical part of the velocity distribution was determined as follows. In general, aircraft flying in the low and middle troposphere made radial passes through hurricanes aiming to obtain "clover leaves" with three symmetrically spaced radial cross sections. Some missions were beautifully executed; on others the flight plan could not be executed fully for a variety of reasons. The cases cited above had sufficiently well distributed radial legs for quantitative evaluation. Information on the upper troposphere was supplied by missions of B-47 aircraft flying at 235-250 mb. as already mentioned.

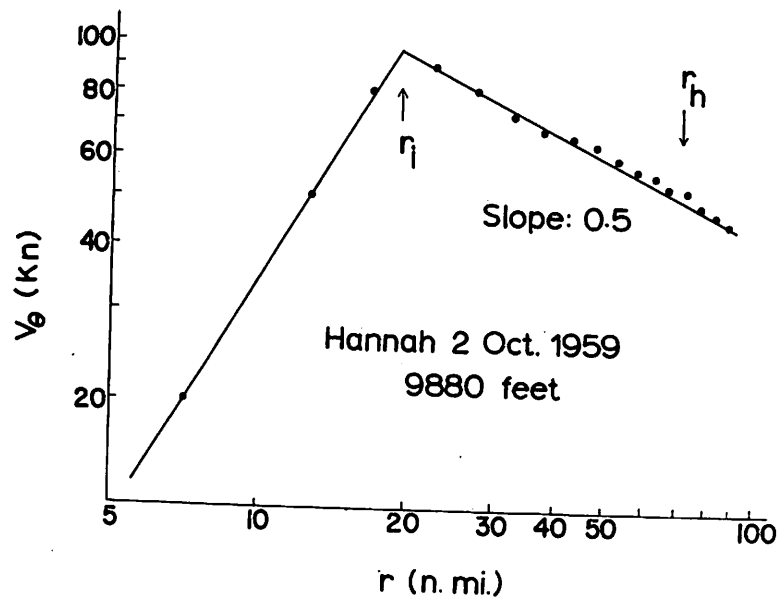


Figure 10. - Tangential speed (kt.) against radius (n.mi.) symmetrical part of wind field on October 2, 1959.

Along each flight leg detailed wind profiles, supplied by the National Hurricane Research Project, were averaged over radial intervals of 5 n.mi. Then a weighting factor was assigned to each leg depending on the area it represented. Given, for instance, three legs with azimuth of 20° , 100° , and 150° , the weight of the middle leg is $(40^\circ + 25^\circ)/360^\circ = .18$. Using the weighting factors so defined, the mean wind speed for each radial interval of 5 n.mi. was found and plotted on log-log paper against radius. Omitting minor wiggles, straight lines were fitted to the distribution of points except where a definite change of slope was in evidence. The profile for hurricane Hannah (fig. 10) is an excellent example of wind distribution with slope that fulfills equation (12) exactly. In passing, it may be mentioned that solid rotation with $v_\theta/r = \text{constant}$ gave a good approximation to the velocity distribution inside the ring of strongest wind in most cases. Such a relation has been noted variously in the literature.

Isotach analysis of maps was used only to extend the profiles outward 5 or 10 n.mi. when one or two legs were a little shorter than the others. In hurricane Helene the maximum wind was established from a single north-south pass, since the flight yielding most data did not penetrate inward of the 20 n.mi. radius. No high-tropospheric flights were conducted successfully in hurricane Donna. But this storm passed through the West Indies rawinsonde network for three days in nearly steady state, so that the upper velocity distribution could be determined to a first approximation by compositing the balloon data relative to the hurricane center. Several data sources had to be used for specification of $v_{\theta 0}$ since the research flights in general operated well inside of r_0 .

Another difficulty lies in the fact that only a first approximation to r_0 can be determined. The outflowing mass rises at least to r_0 , whereas the missions are made on constant pressure surfaces. In hurricane Daisy for instance, the Stokes stream function representing motion in the r - z plane showed ascent intersecting the B-47 flight level (Riehl and Malkus [11]). We need to know θ_e and the motion field in vertical cross section for precise specification of r_0 . Excepting hurricane Daisy, however, the laborious construction of such cross sections has not been undertaken. Hence we must make a best estimate from rawinsonde or B-47 flight data noting that r_0 must be equal to or smaller than the radius at which $v_\theta = 0$ at the B-47 flight level.

We now pass to the examination of individual cases; for this purpose we shall adopt knots (kt.) and nautical miles (n.mi.) as speed and distance units.

Hurricane Donna: This is the most severe hurricane investigated by NHRP during the period 1956-62. Extreme winds close to 150 kt. were measured by aircraft and also at landfall in the Florida Keys. On several days, notably on September 7, 1960, research aircraft penetrated this hurricane. On that day, the author investigated the storm in an A3-D Navy jet research plane at pressure altitudes between 35,000 and 43,000 ft. Unfortunately the instruments did not work properly, so that a reliable record was not obtained. As the best obtainable substitute, the velocity distribution at 45,000 ft. from the 60 n.mi. radius outward, composited from the rawin data of the West Indies network, is shown in figure 11. The pattern is rather spectacular and typical of the upper wind field on which much of the reasoning in this paper is based.

The level is high enough to have been crossed by the main outflow in the region covered by data. We find that $r_0 = 140$ n.mi.; from similar compositing at 1,000 ft., $v_{\theta 0} = 35$ kt. The profile of the tangential component of velocity given by the aircraft data (fig. 12) is well approximated by equation (12). At r_0 , values of $v_{\theta 0}$, as given by the 1,000-ft. winds and by extrapolation of the profile with slope of 0.5, differ only slightly. The following quantities are obtained: $r_i = 20$ n.mi., $v_{\theta i} = 110$ kt. $r_h = 90$ n.mi., $v_{\theta i}$ from heat source = 100 kt. Herewith balance is obtained using the model as closely as can be expected. Actually Donna continued to travel in steady state until landfall on September 10.

Hurricane Daisy: This hurricane, moving slowly northward east of Florida, was within easy reach of the NHRP aircraft; successful penetrations were made on no less than four successive days. Riehl and Malkus [10] have performed various balance calculations for this case, including that of absolute angular momentum. They found that on the day of peak intensity (August 27, 1958) it was necessary to postulate some export by small-scale lateral stresses for balance. This postulate, however, was enforced by the use of drag coefficients, calculated from the heat budget, which averaged substan-

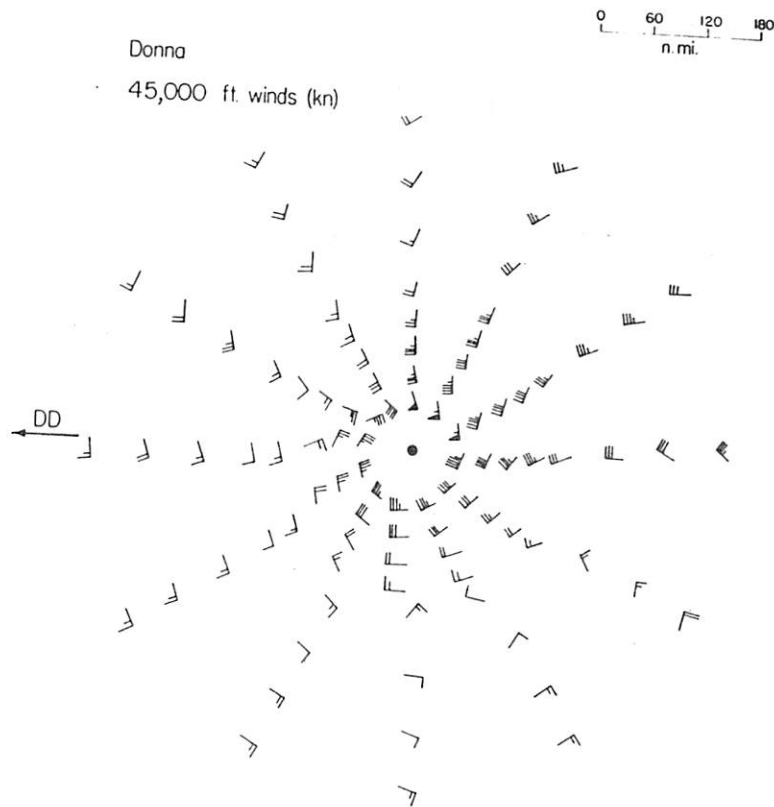


Figure 11. - Winds at 45,000 ft. (kt.) relative to hurricane Donna, composited from West Indies rawin observations September 6-9, 1960. Inner radius 60 n.mi.; outer radius 300 n.mi.

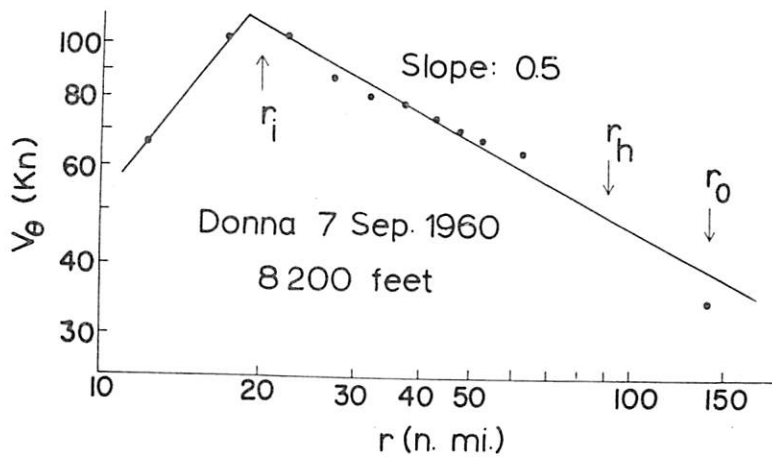


Figure 12. - Radial profile of tangential component of velocity, hurricane Donna, September 7, 1960.

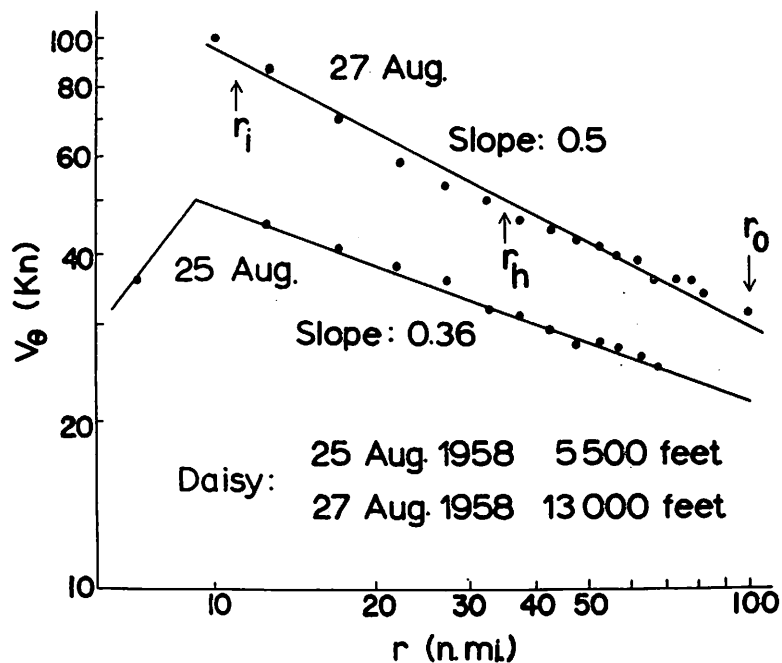


Figure 13. - Radial profiles of tangential component of velocity for hurricane Daisy August 25 and 27, 1958.

tially below 2.5×10^{-3} . As already noted, much uncertainty is attached to such calculations since direct measurements of momentum transfer from air to ocean in hurricanes have not been made. We shall now compute our parameters with the present model which does not include lateral eddy momentum transport.

Flights in the lower troposphere were conducted by R. C. Gentry and the author on August 25 and by R. H. Simpson on August 27. On both days the tangential velocity component profile can be approximated by $v_{\theta} r^x = \text{const}$ (fig. 13). The slope was weak on August 25 when hurricane force was first attained; on August 27 equation (12) holds. On that day (from fig. 26 in [11]) $r_o = 100$ n.mi. and $v_{\theta o} = 30$ kt. Then $r_i = 11$ n.mi., $v_{\theta i} = 90$ kt., $r_h = 35$ n.mi. and $v_{\theta i}$ from heat source = 84 kt. Within the limits of the model, balance exists approximately. It is of interest that Daisy's intensity began to diminish almost immediately. A considerably weaker profile was measured on August 28 in the last mission into this hurricane by the author (fig. 14).

Daisy is the only hurricane where, from [10] the relation between upper and lower height gradients can be partly checked. Between the 15 n.mi. and 80 n.mi. radii, which do not correspond exactly to r_i and r_o , the height difference was 350 m. in the layer surface to 900 mb., and 170 m. in the layer from 400 to 200 mb., where, presumably, the main outflow occurred.

Figure 14. - Radial profile of tangential component of velocity for hurricane Daisy August 28, 1958.

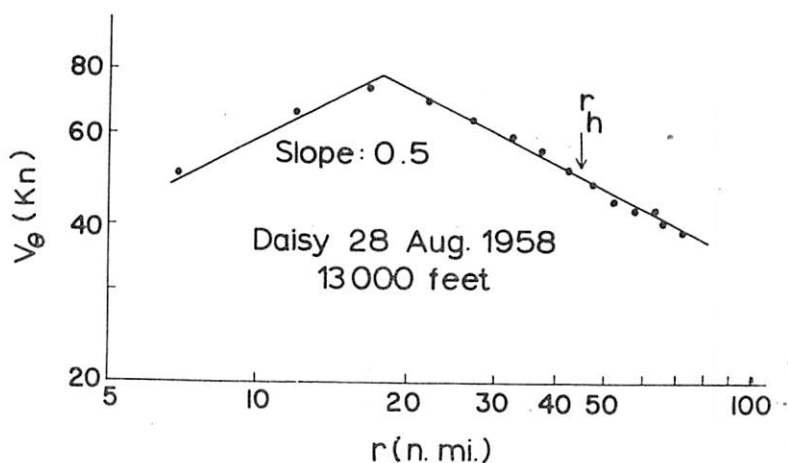
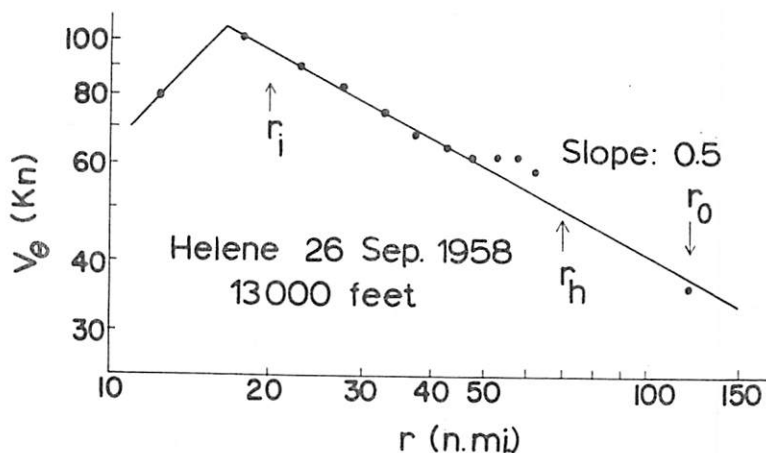


Figure 15. - Radial profile of tangential component of velocity for hurricane Helene, September 26, 1958.



Hurricane Helene: Successful missions into this hurricane were made on September 24, 25, and 26, 1958 as it approached the Carolina coast of the United States from the southeast. The B-47 flew only on September 26, the day of peak intensity. R. C. Gentry conducted the missions of the lower aircraft; this profile (fig. 15) again fits equation (12). The velocity distribution from B-47 data extends to the 100 n.mi. radius. Extrapolating to $v_{\theta} = 0$, $r_0 = 120$ n.mi. For the lower atmosphere there were no data at this radius. An approximation was obtained from the surface isotach analysis by Schauss [12] for 0600 GMT, September 27. His data, for the eastern half of the storm, yield $v_{\theta 0} = 36$ kt., a value which fits extrapolation of the profile of figure 15. Accepting these values as best estimates, $r_i = 20$ n.mi., $v_{\theta i} = 95$ kt. $r_h = 70$ n.mi., $v_{\theta h}$ from heat source = 94 kt. Again, there is balance. We note, however, that the fit is a little poorer than in the two preceding cases. The difficulties of proper estimation of boundary conditions may be at fault, especially that of r_0 which is harder to obtain for Helene than for Donna or Daisy. Judging from the radial temperature distribution measured by

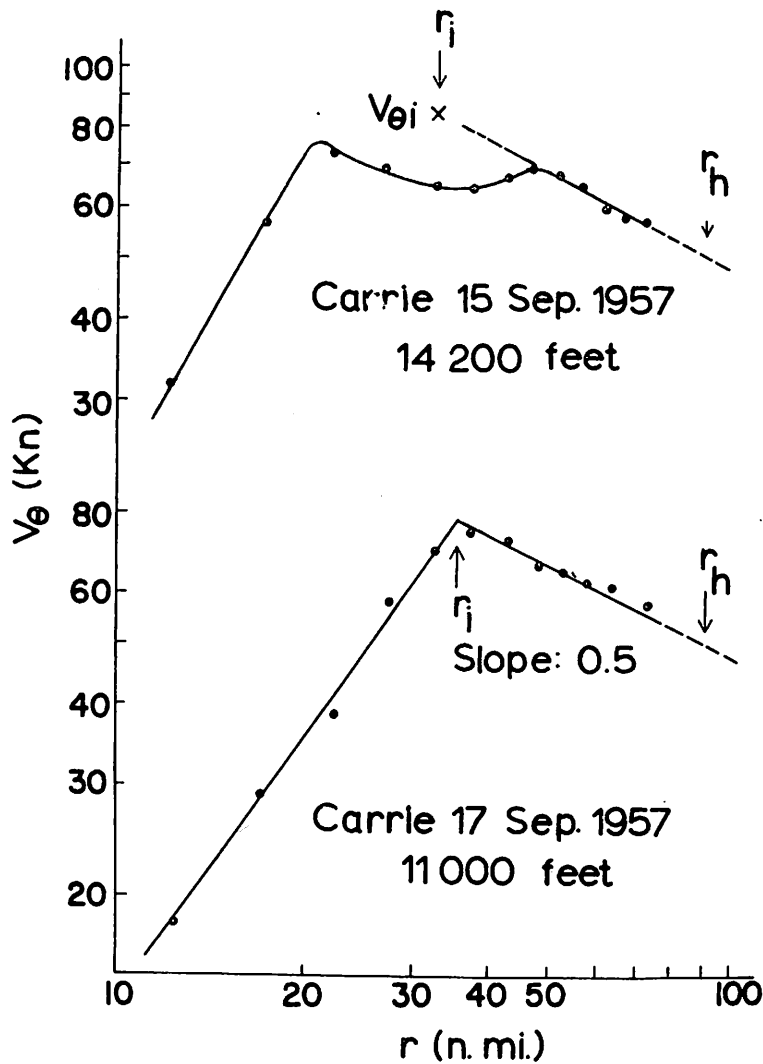


Figure 16. - Radial profile of tangential component of velocity for hurricane Carrie, September 15 and 17, 1957.

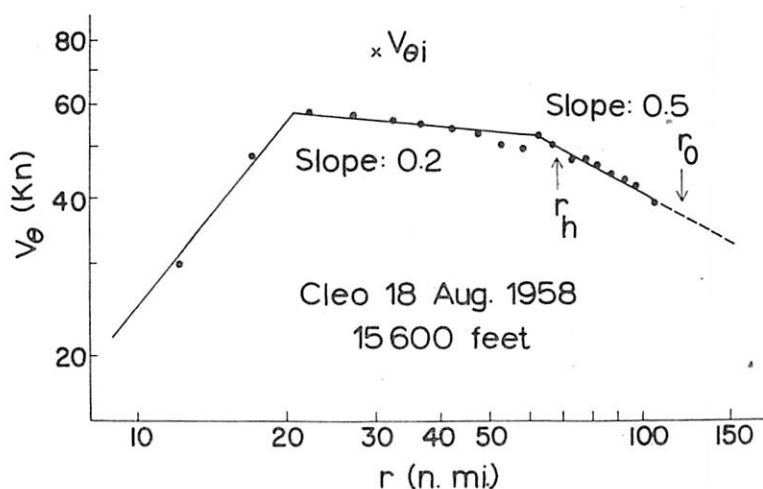
the B-47, the principal outflow layer must have crossed the flight level fairly close to the eye; hence r_o may well be overestimated.

In both Daisy and Helene the B-47 made successful passes through the quadrant with strongest wind. Speeds of the strength measured at low levels were not encountered in either case. Observed speeds indicate that the ring of maximum wind had moved outward 3-4 n.mi. from r_i when the air in the eye wall was crossed by the B-47.

Hurricane Carrie: This hurricane was investigated first by R. H. Simpson while it was moving northwestward south of Bermuda. Two days later, when it was recurving toward east on a clockwise path around Bermuda, Simpson made a second set of traverses. The B-47 data are rather weak and do not cover the hurricane well. As a best estimate, $v_\theta = 0$ at $r = 160$ n.mi. on both days.

Again this may be an overestimate; but we shall accept it lacking more complete data in the mass outflow. There are no observations measuring $v_{\theta 0}$; in this case we must assume that the $v_\theta r^{1/2} = \text{const}$ profile holds as far as r_o . A profile with this slope is observed on September 17 and in the outer region on September 15; the constant is the same on both days (fig. 16). The profile

Figure 17. - Radial profile of tangential component of velocity for hurricane Cleo, August 18, 1958.



in the inner region is quite remarkable on September 15 though by no means unique (found, for instance, in Esther of 1961). The hurricane although apparently approaching the $v_{\theta} r^{1/2}$ profile, for some reason had not achieved it at the time of the measurements.

Given $r_0 = 160$ n.mi., $v_{\theta 0} = 38$ kt. Parameters are as follows on September 15: $r_i = 33$ n.mi., $v_{\theta i} = 80$ kt., $r_h = 90$ n.mi., $v_{\theta i}$ from heat source = 90 kt. From these calculations and the slope of the profile in figure 16 we may suppose that the hurricane is not in steady state; the model, of course, does not predict what changes will occur. Actually the outer velocity field propagated inward during the next two days while the inner maximum died out. By September 17 a profile corresponding closely to the model had been established; this includes all parameters.

Hurricane Cleo: This hurricane was recurving into the westerlies in the Atlantic east of Bermuda on a fairly rapid northward path when it was intercepted by N. E. LaSeur on August 18, 1958 near 35° N. A highly successful three-level mission was conducted that day. From the B-47 record the best estimate for r_0 is 120 n.mi. With only a short extrapolation of the lower tangential speed profile (fig. 17) $v_{\theta 0} = 36$ kt. The profile of figure 17 resembles that of Carrie for September 15, 1957. Again we see a tendency for establishment of the $v_{\theta} r^{1/2}$ profile in the outer region, which is unable to penetrate inward and produce a really strong hurricane. At the radius of strongest wind the symmetrical part of the velocity field falls short of hurricane intensity by a good margin; observed maximum speeds were somewhat above 80 kt. Our computations are hardly applicable to this case since the location of r_0 is not determined entirely by the processes postulated in this paper. Nevertheless, as a matter of interest, we obtain $r_i = 30$ n.mi. in view of the high latitude and $v_{\theta i} = 75$ kt. Because of the proximity of r_h to the terminal radius of the outer profile, the heat source calculation is best omitted. No doubt, however, there was a substantial oceanic heat source acting in the sec-

tor with hurricane-force wind. On the whole it is clear that the structure of Cleo is not explained by the model.

8. SUMMARY

The observed and computed quantities just described for six hurricane days are summarized in Table 1. In these cases and in others (figs. 10, 14) the v_{θ} -profile could be fitted readily with a straight line with slope of 0.5. This fact was not known when equations (10) and (12) were first considered for the model. Validity of the principle of conservation of potential vorticity appears to be rather well demonstrated.

Computed values of r_i are somewhat larger than those obtained from the v_{θ} -profiles. The differences, hardly significant on four days, could stem from overestimates of r_o . Calculated values of $v_{\theta i}$ from the heat source fall somewhat short of observed values on the four days with approximate balance. In view of the somewhat arbitrary choice of $v_{\theta h}$ and E it is not advisable to make further deductions about the differences between observed and computed maximum wind, although table 1 contains some material for speculation.

On the whole the crude model studied gives a rather fair approximation to four out of six hurricanes, especially the strong ones. Additional evidence, given in figures 1 and 6-8, supports the model. It is seen that symmetrical vortex calculations are useful for describing some important structural features of certain fully developed hurricanes. It must be emphasized that a complete theory has not been attempted. For that, it would be necessary to include important features of the asymmetric part of hurricane structure, such as those noted by Gray [2].

Because of the role assigned to the outer boundary condition in the model it will be of interest to study to what extent variations on that boundary are related to variations in hurricane intensity. Changes on the boundary may be impressed by neighboring circulations, especially those outside the Tropics. From empirical studies the author has formed the opinion that hurricanes cannot be regarded as fully isolated vortices and that they may be influenced strongly by external circulation (for instance, see Riehl [9]). Further computations on this subject are in progress.

Table 1. - Summary of hurricane parameters.

	Observed				Computed			Slope of v_{θ} -profile
	r_o n.mi.	$v_{\theta o}$ kt.	r_i n.mi.	$v_{\theta i}$ kt.	r_i	$v_{\theta i}$ (mom.)	$v_{\theta i}$ (heat)	
Donna, Sept. 7, 1960	140	38	18	110	20	110	100	0.5
Daisy, Aug. 27, 1958	100	30	10	95	11	90	84	0.5
Helene, Sept. 26, 1958	120	36	17	105	20	95	94	0.5
Carrie, Sept. 15, 1957	160	38	21	75	33	80	90	
Carrie, Sept. 17, 1957	160	38	35	77	37	75	73	0.5
Cleo, Aug. 18, 1958	120	36	21	58	30	75	--	

ACKNOWLEDGMENT

The author wishes to thank Drs. Ferdinand Baer and Michio Yanai for their critical review of the manuscript and for various discussions of the subject matter. Mr. Russel Elsberry and Mr. Richard King performed many of the computations. The research was conducted under a contract between the United States Weather Bureau and Colorado State University.

REFERENCES

1. M. Ausman, "Some Computations of the Inflow Angle in Hurricanes Near the Ocean Surface," Department of Meteorology, University of Chicago, 1959 (multigraphed). (Contract N505i-02036 Project NR-082-120.)
2. W. M. Gray, "On the Balance of Forces and Radial Accelerations in Hurricanes," Quarterly Journal of the Royal Meteorological Society, vol. 88, No. 378, Oct. 1962, pp. 430-458.
3. B. Haurwitz, "The Height of Tropical Cyclones and of the 'Eye' of the Storm," Monthly Weather Review, vol. 63, No. 2, Feb. 1935, pp. 45-49.
4. C. L. Jordan, "Mean Soundings for the West Indies Area," Journal of Meteorology, vol. 15, No. 1, Feb., 1958, pp. 91-97.
5. E. Kleinschmidt, "Grundlagen einer Theorie der tropischen Zyklonen," Archiv für Meteorologie, Geophysik und Bioklimatologie, Serie A, vol. 4, 1951, pp. 53-72.
6. D. W. Krueger, "A Relation Between the Mass Circulation Through Hurricanes and Their Intensity," Bulletin of the American Meteorological Society, vol. 40, No. 4, Apr. 1959, pp. 182-189.
7. J. S. Malkus and H. Riehl, "On the Dynamics and Energy Transformations in Steady-State Hurricanes," Tellus, vol. 12, No. 1, Feb. 1960, pp. 1-20.
8. E. Palmén and H. Riehl, "Budget of Angular Momentum and Energy in Tropical Cyclones," Journal of Meteorology, vol. 14, No. 2, Apr. 1957, pp. 150-159.
9. H. Riehl, "On the Formation of West-Atlantic Hurricanes," Department of Meteorology, University of Chicago, Miscellaneous Report No. 24, Part I. 1948.
10. H. Riehl, Tropical Meteorology, McGraw-Hill Book Co., Inc., New York, 1954, 392 pp.
11. H. Riehl and J.S. Malkus, "Some Aspects of Hurricane Daisy, 1958," Tellus, vol. 13, No. 2, May 1961, pp. 181-213.
12. C.E. Schauss, "Reconstruction of the Surface Pressure and Wind Fields of Hurricane Helene," National Hurricane Research Project Report No. 59, U. S. Weather Bureau, 1962, 45 pp.